

Multi-Level Representation for the Control Design of a Super Capacitor Storage System for a Microgrid Connected Application

P. LI^{1,2}, Ph. Degobert², B. François¹ and B. Robyns³

Laboratoire d'Electrotechnique et d'Electronique de Puissance de Lille (L2EP)

¹ Ecole Centrale de Lille, Cité Scientifique, BP 48, 59651 Villeneuve d'Ascq Cedex, France

² Ecole Nationale Supérieure d'Arts et Métiers, 8 Boulevard Louis XIV, 59046 Lille Cedex, France

³ Hautes Etudes d'Ingénieur, 13 Rue de Toul, 59046 Lille Cedex, France

e-mail: lephis@gmail.com, philippe.degobert@lille.ensam.fr, bruno.francois@ec-lille.fr, benoit.robyns@hei.fr

Abstract. In this paper an average multi-level representation of power electronic converters is used to design a dynamic model of a Super Capacitor Bank for a microgrid application. A dedicated multi-level modeling is designed to quantify energy variations in storage elements (super capacitors, DC bus) and various losses. We demonstrate that this model is sufficient to design the control system of the entire power storage system, meanwhile the super capacitors, the chopper and the grid connected converter. The proposed global model is simulated with the help of Matlab-SimulinkTM by considering two units of 48V 144F super capacitor modules.

Key words

Super Capacitor Bank, microgrid, distributed generation, control design, multi-level representation.

1. Introduction

A microgrid is a possible future energy system structure, which is based on small generation plants (photovoltaic, micro-turbine, fuel cells, etc.), together with storage devices (super capacitors (SC), batteries and flywheels for example), and controllable loads [1][2]. Such systems can be interconnected to a low voltage distribution system or islanded. The advantage of the microgrid concept lies in a significant reduction of CO₂ emissions for the following reasons [2]:

- The closed use of both electricity and heat increases the overall energy efficiency;
- Significant environmental benefits arise from the use of low or zero emission generators including PV arrays and fuel cells;
- Low impact on the electricity grid by a good match between generation and load, despite a potentially significant level of intermittent resemble energy based sources.

Fig. 1 shows the studied hybrid system: a 17.3kWpeak photovoltaic system composed of six groups of 18 PV arrays. This PV power plant is associated with a 28kWelectric Capstone micro turbine and a 72F/96V Maxwell Super Capacitor Bank (SCB). This hybrid system has been installed at the laboratory L2EP-ENSAM Lille [3][4]. A great interest of the power storage is that the super capacitor has a quick dynamic response time to reduce the power variation in the microgrid. The multi-level representation has been

developed in order to propose a synthetic and dynamical description of the electromechanical conversion systems for microgrid applications. This description is an expansion of the Energetic Macroscopic Representation (EMR) [5] and allows the subdivision of the whole complex system into simple blocks, which yield a synthetic and physical representation. The expansion by multi-level representation integrates a power flow level, a power calculation level and their corresponding control levels, since the power flow is the most important factor for the supervision of microgrid units. A Maximal Control Structure can be deduced from the multi-level modeling through specific inversion rules. This results in a theoretical control structure with many operations and measurements.

In the second part of this paper, the SCB power storage system is modeled by using a graphical representation of all exchanged physical quantities and power flows. In the third part, control tasks of the storage system are explained and implementations of control functions are detailed. The fourth part enables the supervision of the real power, which is integrated into the microgrid center controller (Local Supervision in fig. 1). This center controller helps the SCB to calculate its real power reference. The proposed global model is simulated with the help of Matlab-SimulinkTM.

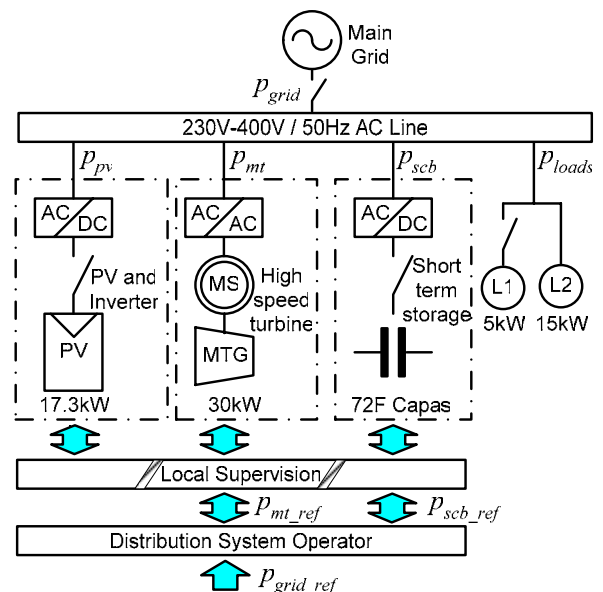


Fig. 1: PV/MTG/Super capacitor Microgrid scheme

2. SCB multi-level modeling

A. Maxwell 48V/144F super capacitor module

A SCB is useful for the compensation of fluctuation powers since it is capable of controlling both real and reactive powers for the benefit of power quality. It handles an Electric Double Layer Capacitor (EDLC) module with power electronic converters.

The 144F/48V EDLC is a self-constrained energy storage device, storing up to 161kJ (44.8W.Hr) of energy. It includes eighteen individual super capacitor cells, bus bar connections, and an integral active cell balancing circuitry [6]. Two modules are connected in series to obtain higher operating voltage and storage energy for our microgrid application. The module characteristics are shown in Tab. 1.

Tab. 1. Parameters of the used EDLC

Parameters	Value
Capacitance (C_0)	144F + 20%, initial
Voltage	48.6 Volts DC Max.
DC Resistance (R_s)	11 mΩ Max., initial

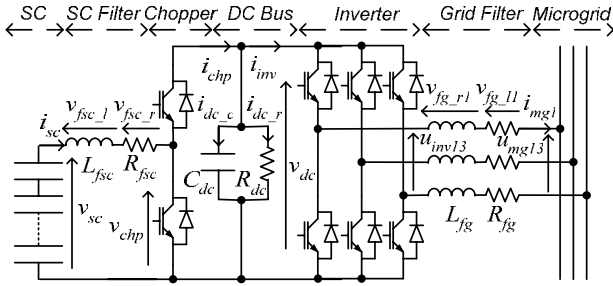


Fig. 2: Electric scheme of the SCB

B. Step 1: EMR level modeling

The SCB is composed of the Super Capacitor (SC), a SC filter, a chopper, a DC bus, an inverter and a three-phase grid filter (fig. 2). The first step of the SCB multi-level modeling is consists to gather dynamical equations of each element into 'ProX' and 'ES' macro blocs in order to obtain an EMR (fig. 4, EMR level).

1) Modeling of the SC (macro bloc 'Pro1')

The super capacitor module is modeled as a voltage source. For the study of power system applications, the model of Zubieta and Bonert [7] can be applied. Nevertheless, for the simplification of the study, the model with a resistor R_s and a ideal capacitor C_0 in series is used.

$$\frac{dv_C}{dt} = \frac{1}{C_0} i_{sc} \quad (1)$$

$$v_R = R_s i_{sc} \quad (2)$$

$$v_{sc} = v_C + v_R \quad (3)$$

2) Modeling of the filter ('Pro2')

The SC filter is modeled as an inductance (L_{fsc}) and a resistance (R_{fsc}) in series.

$$\frac{di_{sc}}{dt} = \frac{1}{L_{fsc}} v_{fsc_l} \quad (4)$$

$$v_{fsc_l} = v_{sc} - v_{chp} - v_{fsc_r} \quad (5)$$

$$v_{fsc_r} = R_{fsc} i_{sc} \quad (6)$$

3) Modeling of the chopper ('Pro3')

The chopper adapts the low voltage across the super capacitor to the desired voltage for the DC bus. An equivalent continuous model [8] of the chopper is used by a mean value modulation function m_{chp} :

$$\begin{cases} v_{chp} = m_{chp} v_{dc} \\ i_{chp} = m_{chp} i_{sc} \end{cases}, m_{chp} \in [0,1] \quad (7)$$

4) Modeling of the grid-side DC bus ('Pro4')

The DC bus is considered as a capacitor (C_{dc}) and a resistance (R_{dc}) in parallel.

$$\frac{dv_{dc}}{dt} = C_{dc} i_{dc_c} \quad (8)$$

$$i_{dc_c} = i_{chp} - i_{inv} - i_{dc_r} \quad (9)$$

$$i_{dc_r} = \frac{1}{R_{dc}} v_{dc} \quad (10)$$

5) Modeling of the inverter ('Pro5')

An equivalent mean modeling of the power converters [8] is sufficient for the study. It represents fundamental phase-to-phase voltage $\underline{u}_{inv} = [u_{inv13}, u_{inv23}]^T$ and line currents $\underline{i}_{mg} = [i_{mg1}, i_{mg2}]^T$ components as:

$$\underline{u}_{inv} = \underline{m}_{inv} \cdot v_{dc} \quad (11)$$

$$i_{inv} = \underline{m}_{inv}^T \cdot \underline{i}_{mg} \quad (12)$$

where $\underline{m}_{inv} = [m_{inv1}, m_{inv2}]^T$ is the modulation index vector. Line voltages $\underline{v}_{inv} = [v_{inv1n}, v_{inv2n}]^T$ are obtained by:

$$\underline{v}_{inv} = \frac{1}{3} \begin{bmatrix} 2 & -1 \\ -1 & 2 \end{bmatrix} \cdot \underline{u}_{inv} \quad (13)$$

6) Modeling of the three-phase filter ('Pro6')

The line current \underline{i}_{mg} are deduced from the inverter voltages \underline{u}_{inv} and the grid voltages $\underline{u}_{mg} = [u_{mg13}, u_{mg23}]^T$.

$$\frac{d}{dt} \underline{i}_{mg} = \frac{1}{L_{fg}} \underline{v}_{fg_l} \quad (14)$$

$$\underline{v}_{fg_l} = \frac{1}{3} \begin{bmatrix} 2 & -1 \\ -1 & 2 \end{bmatrix} (\underline{u}_{inv} - \underline{u}_{mg}) - \underline{v}_{fg_r} \quad (15)$$

$$\underline{v}_{fg_r} = R_{fg} \underline{i}_{mg} \quad (16)$$

where L_{fg} and R_{fg} are the inductance and resistance of the filter, the $\underline{v}_{fg_l} = [v_{fg_l1}, v_{fg_l2}]^T$ and $\underline{v}_{fg_r} = [v_{fg_r1}, v_{fg_r2}]^T$ are the voltages respectively across L_{fg} and R_{fg} .

7) Modeling of the microgrid ('ES')

The grid voltages \underline{u}_{mg} is modeled by :

$$\underline{u}_{mg} = \begin{bmatrix} u_{mg13} \\ u_{mg23} \end{bmatrix} = \sqrt{2} A \begin{bmatrix} \sin(2\pi ft - \pi/6 + \theta_0) \\ \sin(2\pi ft - \pi/2 + \theta_0) \end{bmatrix} \quad (17)$$

where A is the rms value of the grid phase-to-phase voltage, f is the grid frequency and θ_0 is the initial angle of the grid voltage. The line currents \underline{i}_{mg} are considered as disturbances for the microgrid.

C. Sept 2: Power calculation level

The second step for the multi-level modeling uses an interface, which is designed to calculate the different powers. They are classified in three terms: the intermediary powers between two elements, the exchanged powers with a storage element, and the losses gathered into the macro blocs named 'IntX' in the 'Power Calculation' level of the fig. 4.

D. Step 3: Power flow representation level

The third step for the multi-level modeling describes the power flow (fig. 3) from the super capacitor modules to the microgrid. The macro blocs, which are named 'PowX' in the 'Power Flow' level of the fig. 4, represent the modeling equations.

For the storage elements (as example the SC filter), the input power (P_{scf} from the SC) is separated into losses (P_{fsc_los}), the exchanged power with the storage unit (P_{fsc_sto}) and the output power (p_{fch}) is expressed as:

$$Pow1: p_{fch} = p_{scf} - p_{fsc_los} - p_{fsc_sto} \quad (18)$$

where p_{fsc_sto} is the total of the accumulation power ($p_{fsc_sto}^+$) and the restitution power ($p_{fsc_sto}^-$).

For the power electronic converters, the input power is equal to the output power since losses are neglected. The power flow from the SC to the microgrid is modeled by the following equations:

$$Pow2: p_{fch} = p_{chb} \quad (19)$$

$$Pow3: p_{bin} = p_{chb} - p_{dc_los} - p_{dc_sto} \quad (20)$$

$$Pow4: p_{bin} = p_{inf} \quad (21)$$

$$Pow5: p_{mgs} = p_{inf} - p_{fg_los} - p_{fg_sto} \quad (22)$$

These power equations are bidirectional. For the SCB, it is possible to perform the accumulation and the restitution of the power.

The complete multi-level modeling of the SCB is composed of three levels: *EMR*, *Power Calculation* and *Power Flow* (fig. 4).

3. Design of the control system

The global system has three control inputs in order to manage the system. The inverter has two independent modulation functions m_{inv1} and m_{inv2} using its switching orders. The chopper has only one modulation function m_{chp} . The control task is to reduce the power variations of the microgrid. The inverter is used to control the real and reactive power at the connection point. The control input of the chopper is used to control DC bus voltage, since the voltage of the DC bus must be constant for correct system performances. The control system is ordered by the following steps according to the rules of the multi-level representation.

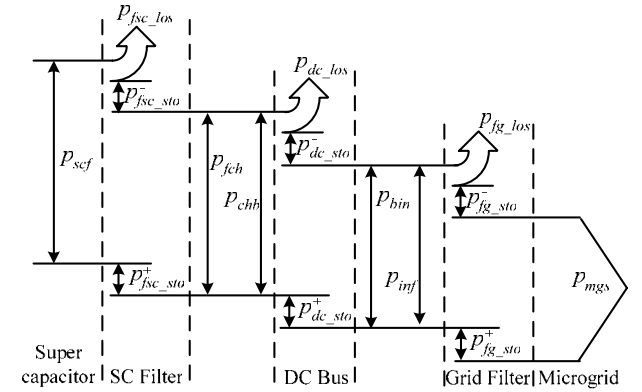


Fig. 3: Power flow from the SC to the microgrid

Tab. 2. Equations of the Power calculation interface.

Intermediary powers	Storage powers	Losses
Int1 : $p_{scf} = v_{sc} i_{sc}$	Int3 : $p_{fsc_sto} = v_{fsc} i_{sc}$	Int2 : $p_{fsc_los} = R_{fsc} i_{sc}^2$
Int4 : $p_{fch} = v_{chp} i_{sc}$	Int7 : $p_{dc_sto} = v_{dc} i_{dc_c}$	Int6 : $p_{dc_los} = v_{dc}^2 / R_{dc}$
Int5 : $p_{chb} = v_{dc} i_{chp}$	Int11 : $p_{fg_sto} = (C_{23} \cdot v_{fg_l})^F \cdot (C_{23} \cdot i_{mg})$	Int10 : $p_{fg_los} = R_{fg} (C_{23} \cdot i_{mg})^F \cdot (C_{23} \cdot i_{mg})$
Int8 : $p_{bin} = v_{dc} i_{inv}$	Where $C_{23} = \begin{bmatrix} 1 & 0 \\ 0 & 1 \\ -1 & -1 \end{bmatrix}$ is the calculation matrix from two line currents to three line currents.	
Int9 : $p_{inf} = u_{inv}^T i_{mg}$		
Int12 : $p_{mgs} = u_{mg}^T i_{mg}$		

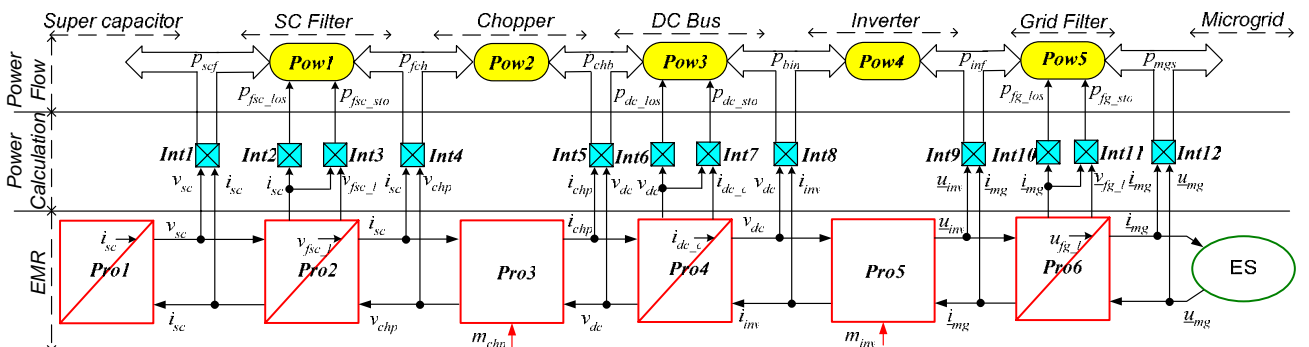


Fig. 4: Multi-level representation of the modeling for a Super Capacitor Bank.

A. Step 4: Mark the stationary quantities and the non-measurable quantities in the EMR level

The SC terminal voltage v_{sc} changes very slowly thanks to a great quantity of stored energy. The DC bus voltage v_{dc} has also a slow dynamic, since it has to be controlled as constant in order to ensure the inverter function. At the ac side, the principal component of all quantities (voltages and currents) is 50 Hz. By modeling them into a 50 Hz rotational Park form, they become stationary. Moreover if their magnitudes are constant, they can be considered constant as \underline{u}_{mg} for the microgrid voltages. In the multi-level representation, the stationary quantities are visualized by the thick solid lines (fig. 6).

The voltages v_{chp} and \underline{u}_{inv} and the currents i_{chp} and i_{inv} are difficult to measure since they are modulated by the converters. These non-measurable quantities are visualized by the thick dashed lines (fig. 6).

B. Step 5: Apply the 'pass' rule and the 'block' rule

This step is necessary to fix the electrical chains. When a macro bloc in the Power Calculation level has a stationary quantity input in the EMR level, it can be used to serve as a possible passage bloc between the EMR level and the Power Flow level. In this condition, this type of macro blocs is colored in the dark blue color. Such as *Int1* is colored in the dark blue for v_{sc} , *Int5*, *Int6*, *Int7* and *Int8* for v_{dc} , *Int12* for \underline{u}_{mg} .

When a non-measurable quantity in the EMR level is used as an input of the macro bloc for the storage element, it is impossible to design the control strategy by the inversion of another chain of this macro bloc without estimator or a corrector which rejects the disturbances. Some symbols \times are added to present the block in the control part. Such as in *Pro2*, the chain $v_{sc} \rightarrow i_{sc}$ is blocked by the modulation quantity v_{chp} , in *Pro4*, the chain $i_{chp} \rightarrow v_{dc}$ is blocked by the modulation quantity i_{inv} , the chain $i_{inv} \rightarrow v_{dc}$ is blocked by the modulation quantity i_{chp} , in *Pro6*, the chain $\underline{u}_{mg} \rightarrow \underline{i}_{mg}$ is blocked by the modulation quantity \underline{u}_{inv} (fig. 6).

C. Step 6: Fix the electrical chains

The multi-level representation helps us to find the electrical chain in the power model level in order to design the control system.

The first electrical chain is used to control the real and reactive power at the connection point to the microgrid by the modulation functions of the inverter. The path from the control input of the inverter to the powers injected to the microgrid is obvious (fig. 6): $m_{inv}(Pro5) \rightarrow \underline{u}_{inv}(Pro6) \rightarrow \underline{i}_{mg}(Int12) \rightarrow p_{mgs}$ and q_{mgs}

The second electrical chain is used to control the DC bus voltage v_{dc} by the modulation function m_{chp} . Since v_{dc} is a stationary quantity which is suitable for the processes of division in the control system (28), the first step of this electrical chain is $m_{chp}(Pro3) \rightarrow v_{chp}$ (fig. 6). Now the arrow is pointed to the left side of the chopper, but the

destination v_{dc} is at its right side. The power flow level is used to establish the relation between v_{chp} and v_{dc} . At the left side of the chopper, there is only one bloc *Int1* for the passage. So the electrical chain is drawn from v_{chp} to i_{sc} in order to reach *Int1*. Since both external currents (i_{chp} and i_{inv}) of the DC bus are modulation quantities, the end of the electrical chain in the power flow level is fixed on the DC bus storage power p_{dc_sto} . Finally the equations *Int7* and *Pro4* are used to reach the DC bus voltage from p_{dc_sto} . The second electrical chain is (fig. 6): $m_{chp}(Pro3) \rightarrow v_{chp}(Pro2) \rightarrow i_{sc}(Int1) \rightarrow p_{sc}(Pow1) \rightarrow p_{fch}(Pow2) \rightarrow p_{chb}(Pow3) \rightarrow p_{dc_sto}(Int7) \rightarrow i_{dc_c}(Pro4) \rightarrow v_{dc}$

D. Step 7: Control the fast dynamic quantities by the inversion of EMR

The control system of fast dynamic quantities is obtained by using inversion rules of equations from the EMR modeling level (fig. 6). Hence a grid current controller (macro bloc '*Pro6c*' in the fig. 6) is required to enslave grid currents to prescribed reference (\underline{i}_{mg_ref}). Two controllers ('*Pro3c*' and '*Pro5c*') are used for power electronic converters. A voltage controller ('*Pro4c*') is used to set the DC bus voltage reference and a current controller ('*Pro2c*') sets the super capacitor current reference (fig. 6). The following sections give the details of each macro control bloc in the 'Control of Dynamic Quantities' level ('*ProXc*') in the fig. 6.

1) Grid connection controller ('*Pro6c*')

A Park transform is used with a synchronization with the first line voltage. In this frame, filter equations are written as:

$$\begin{cases} \frac{di_{mgd}}{dt} = \frac{1}{L_{fg}}(v_{invd} - v_{mgd} - R_{fg}i_{mgd} - L_{fg}\omega_s i_{mgq}) \\ \frac{di_{mgq}}{dt} = \frac{1}{L_{fg}}(v_{invq} - v_{mgq} - R_{fg}i_{mgq} + L_{fg}\omega_s i_{mgd}) \end{cases} \quad (23)$$

The control of these current is obtained by a compensation of grid voltages, a current decoupling and a closed loop control (fig. 5).

2) Inverter controller ('*Pro5c*')

Phase-to-phase voltages are obtained by inversion of the equation (13):

$$\begin{cases} u_{inv13_ref} = v_{inv1_ref} - v_{inv3_ref} \\ u_{inv23_ref} = v_{inv2_ref} - v_{inv3_ref} \end{cases} \quad (24)$$

Modulation functions are calculated by inversion of (11):

$$m_{inv1_ref} = \frac{u_{inv13_ref}}{\hat{v}_{dc}}, \quad m_{inv2_ref} = \frac{u_{inv23_ref}}{\hat{v}_{dc}} \quad (25)$$

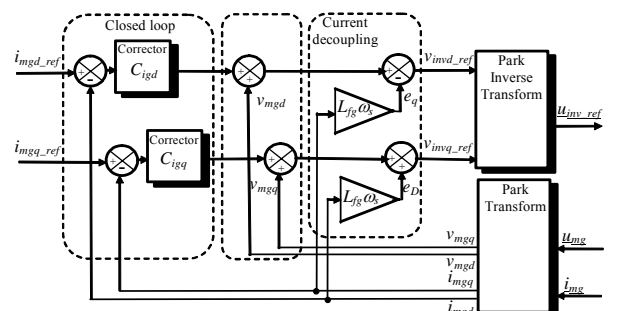


Fig. 5: Grid connection controller (macro bloc '*Pro6c*')

A vector is defined as: $\underline{m}_{inv_ref} = [m_{inv1_ref}, m_{inv2_ref}]^T$. Hence current references can be assumed equal to grid currents.

3) DC bus voltage controller ('Pro4c')

The DC bus voltage is controlled by the current i_{dc_c} (fig. 2).

$$i_{dc_c_reg} = K_{dc_p}(v_{dc_ref} - \hat{v}_{dc}) \quad (26)$$

where K_{dc_p} is the proportional parameter of the corrector for the DC bus voltage control.

4) SC current controller ('Pro2c')

A control loop of the SC current generates the voltage reference of the chopper (v_{chp_reg}) as:

$$v_{chp_reg} = \hat{v}_{sc} - K_{fsc_p}(i_{sc_reg} - \hat{i}_{sc}) \quad (27)$$

where K_{fsc_p} is the proportional parameter of the corrector for the super capacitor current control.

5) Chopper controller ('Pro3c')

The modulation function of the chopper m_{chp_ref} is calculated with the DC bus voltage measurement:

$$m_{chp_ref} = \frac{v_{chp_reg}}{\hat{v}_{dc}} \quad (28)$$

E. Step 7: Power calculation control

The Power Calculation Control level is designed by the inversion or the estimation of the Power Calculation level.

$$Int1c : i_{sc_reg} = \frac{P_{scf_reg}}{\hat{v}_{sc}} \quad (29)$$

$$Int7e : p_{dc_sto_reg} = v_{dc} i_{dc_c_reg} \quad (30)$$

The grid current references are deduced (Int12c) from the equation Int12 for the real power (tab. 2) and the following equation for the reactive power:

$$Q_{mgs} = \frac{1}{\sqrt{3}}((2u_{mg23} - u_{mg13})i_{mg1} - (2u_{mg13} - u_{mg23})i_{mg2}) \quad (31)$$

$$Int12c : \quad (32)$$

$$\begin{cases} i_{mg1_ref} = \frac{(2u_{mg13} - u_{mg23})P_{mgs_ref} + \sqrt{3}u_{mg23}Q_{mgs_ref}}{2u_{mg13}^2 - 2u_{mg13}u_{mg23} + 2u_{mg23}^2} \\ i_{mg2_ref} = \frac{(2u_{mg23} - u_{mg13})P_{mgs_ref} - \sqrt{3}u_{mg13}Q_{mgs_ref}}{2u_{mg13}^2 - 2u_{mg13}u_{mg23} + 2u_{mg23}^2} \end{cases}$$

F. Step 8: Power flow control

The power flow control is obtained by model inversion of the Power Flow level with anticipation of calculated filter losses (\tilde{p}_{fsc_los} and \tilde{p}_{fjg_los}) (tab. 2). The exchanged powers with the filters (p_{fsc_sto} and p_{fjg_sto}) and the losses in the DC bus (p_{dc_los}) are slight enough to be neglected.

$$Pow1c : p_{scf_reg} = p_{fch_reg} + \tilde{p}_{fsc_los} \quad (33)$$

$$Pow2c : p_{fch_reg} = p_{chb_reg} \quad (34)$$

$$Pow3c : p_{chb_reg} = p_{bin_reg} + p_{dc_sto_reg} \quad (35)$$

$$Pow4c : p_{bin_reg} = p_{inf_reg} \quad (36)$$

$$Pow5c : p_{inf_reg} = P_{mgs_ref} + \tilde{p}_{fjg_los} \quad (37)$$

G. Storage level protection

The terminal voltage of the super capacitor represents its energy storage level. For security reasons, it should be between the maximal allowed value and 50% of this value for an efficiency reason.

In order to limit the terminal voltage of the SC, an additional control function has to be used (macro bloc 'SLP' in the Power Supervision level of the fig. 6). For example, if this voltage is under 55V, the available energy for generation decreases in a linear manner (fig. 7). And if this voltage is under 48V (50% of the maximal voltage), the SCB can not operate in a generation mode (fig. 7). The limitation mode for the accumulation mode is designed in the same way (fig. 7).

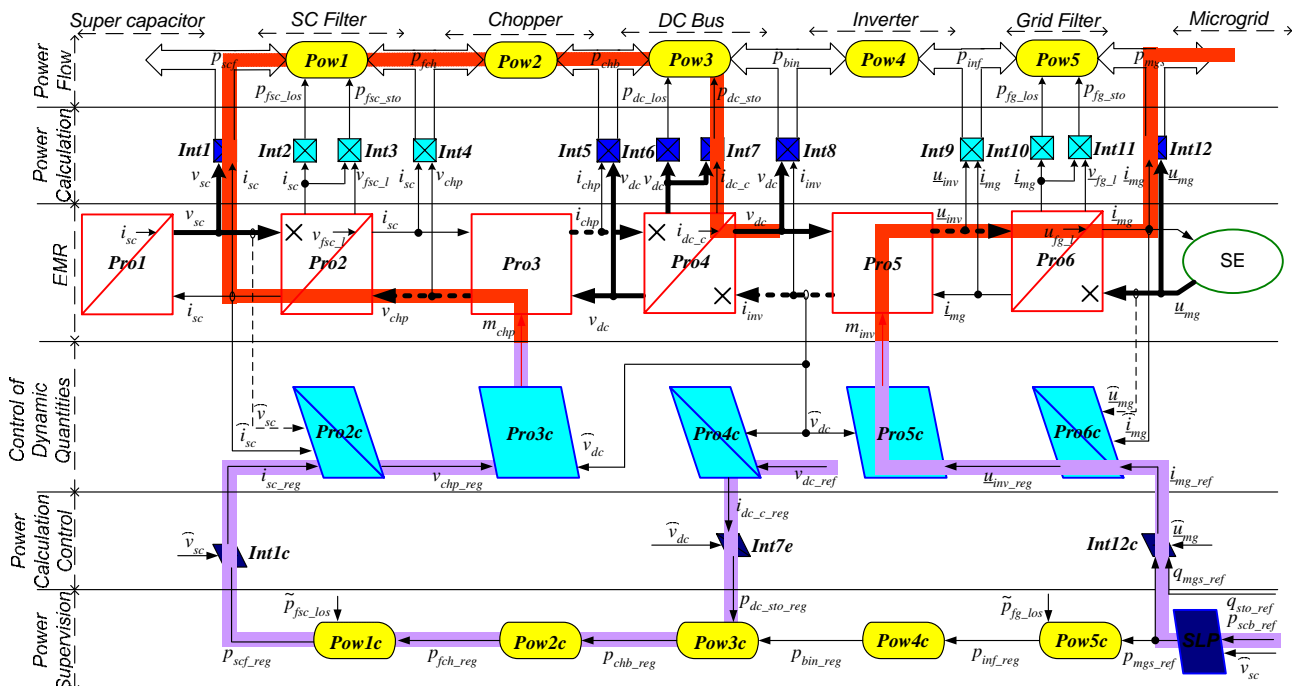


Fig. 6: Control system of the Super Capacitor Bank

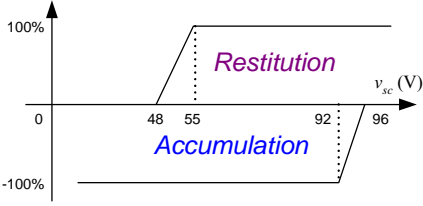


Fig. 7: Energy limitation for the SC storage level

4. Microgrid real power management

The modeling and the control system of the micro turbine and the photovoltaic plant are designed by the same method [9][10]. The coupling of these three systems is performed by the sum of currents at the connection point to the microgrid.

The modeling of the power flow for the microgrid in generation mode can be described by the fig. 8.

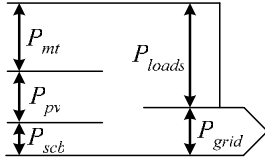


Fig. 8: Power flow for the microgrid in generation mode

The microgrid real power exchanged with the grid p_{grid} is the sum of the micro turbine generation system p_{mt} , the photovoltaic generation system p_{pv} , the SCB p_{scb} and loads p_{loads} (fig. 1).

$$P_{grid}(t) = P_{mt}(t) + P_{pv}(t) + P_{scb}(t) - P_{loads}(t) \quad (38)$$

The micro turbine is used to manage the power in long time range, since it has relatively low dynamics. The average power in a long time range $\{P\}_T$ can be obtained as :

$$\{P\}_T = \frac{1}{T} \int_0^T p(t) dt \quad (39)$$

During such a long time rang, the fast power variations exchanged with the SCB p_{scb} can be neglected. The equation (38) in long time range is expressed as:

$$\{P_{grid}\}_T = \{P_{mt} + P_{pv} - P_{loads}\}_T \quad (40)$$

For a certain microgrid power reference p_{grid_ref} given by the distribution system, the power reference for the micro turbine p_{mt_ref} can be quantified by the inversion of the equation (40) as:

$$\{P_{mt_ref}\}_T = \{P_{grid_ref} - \widehat{P}_{pv} + \widehat{P}_{loads}\}_T \quad (41)$$

In short period, the SCB masters the power flow thanks to its fast response time. The power reference of the SCB p_{scb_ref} can be calculated by the inversion of the equation (38) as:

$$P_{scb_ref}(t) = P_{grid_ref}(t) - \widehat{P}_{mt}(t) - \widehat{P}_{pv}(t) + \widehat{P}_{loads}(t) \quad (42)$$

Another task of the microgrid center controller is to supervise the storage level of the SCB. If its level reaches a high level, a reduction of the active power generated by

the micro turbine can be used. Hence more power will be extracted from the SC and will reduce the stored energy.

$$e_{sc_ref}(t) = \int \Delta p_{mt}(t) dt \quad (43)$$

$$\Delta p_{mt_ref}(t) = k_{pe} (e_{sc_ref}(t) - \widehat{e}_{sc}(t)) \quad (44)$$

$$P_{mt_ref}(t) = P_{grid_ref}(t) - \widehat{P}_{pv}(t) + \widehat{P}_{loads}(t) + \Delta p_{mt_ref}(t) \quad (45)$$

The control strategies presented in this part is integrated to the center supervision bloc of the DSO.

5. Simulation results

Fig. 9 represents experimental variations of the real power and the SC voltage of the studied microgrid.

In order to evaluate our model we simulate it with two real power steps (at 40s and 100s) of the total microgrid loads (fig. 9.a). The photovoltaic power plant generation is set to the Maximal Power Point Tracking (fig. 9.b), which is proportional with the irradiance. The microgrid power generation reference is set to one real power step (at 150s, fig. 9.c), and the sensed power between the microgrid and the main is very close to the power reference, which is given by the Distribution System Operator. The microgrid power measurement is well followed by his reference (fig. 9.c). At 40s and 100s there are two peaks, which generated by the sudden connection and disconnection of a 5kW load, but later the microgrid power is corrected quickly by the SCB. We notice that the micro turbine tries to slowly compensate the fluctuations of the difference between the microgrid reference power and all the passive power variations of the microgrid (PV power and total loads) (fig. 9.d).

We can observe the fast power fluctuations due to the slow response time of the micro turbine are reduced by the short term energy storage system – SCB (fig. 9.e). The SC terminal voltage is well controlled between 48V and 96V (fig. 9.f).

6. Conclusion

A multi-level representation method to design the control system of a SCB is presented in this paper. It is composed of three modeling levels (*EMR*, *Power Calculation* and *Power flow*) and three corresponding control levels (*Control of Dynamic Quantities*, *Power Calculation Control* and *Power Supervision*). The interest of this multi-level representation method is the facility and the quickness for the control design, which uses the power flow for microgrid applications. The real power dispatching algorithm in the microgrid center supervision bloc is detailed in order to clarify the SCB power reference calculation. The simulations results validate this particular control design.

Acknowledgement

This work has been supported by the French National Agency of the Research (ANR SuperEner Project).

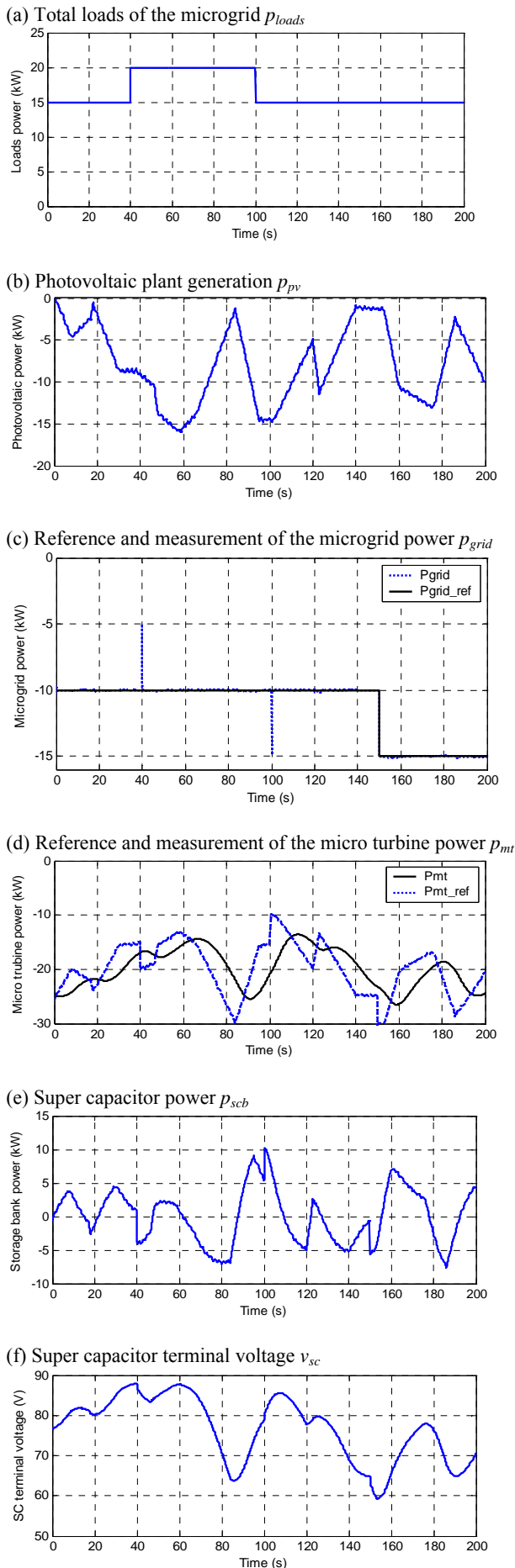


Fig. 9: Simulation results

References

- [1] R. Lasseter, A. Akhil, C. Marnay, J. Stephens, J. Dagle, R. Guttromson, A. Sakis Meliopoulos, R. Yinger, and J. Eto, Integration of Distributed Energy Resources – The MicroGrid Concept, CERT MicroGrid Review, Feb 2002.
- [2] Abu-Sharkh S. et al., Can microgrids make a major contribution to UK energy supply?, Renewable and Sustainable Energy Reviews, 10, (2006), pp. 78-127.
- [3] Ph. Degobert, S. Kreuawan, X. Guillaud, Micro-grid powered by photovoltaic and micro turbine, International Conference on Renewable Energy and Power Quality (ICREPO'06), CD-ROM, Palma de Mallorca, Spain, April, 2006
- [4] Ph. Degobert, S. Kreuawan, P. Li, B. François, Reduction of Fast Fluctuations of Power in a Microgrid with Super Capacitors, ESSCAP'06, CD-ROM, Lausanne, Switzerland, Nov. 2006.
- [5] A. Bouscayrol, Ph. Delarue, X. Guillaud, Power strategies for maximum control structure of a wind energy conversion system with a synchronous machine, Renewable Energy, vol. 30, pp. 2273-2288, May 2005.
- [6] Maxwell technologies application note, How to determine the appropriate Size Ultracapacitor for your application, document 1007236, Rev 2, October 2004.
- [7] L. Zubieta, and R. Bonert, Characterization of double-layer capacitors for power electronics applications, IEEE Trans. Ind. Appl., Vol. 36, no. 1, pp. 199-205, 2000.
- [8] B. Robyns, Y. Pankow, L. Leclercq, B. François, Equivalent continuous dynamic model of renewable energy system, Proceedings of the 7th International Conference on Modeling and Simulation of Electric Machines, Converters and systems, ELECTRIMACS 2002, Montreal, Aug., 2002.
- [9] P. Li, Ph. Degobert, B. François, B. Robyns, Multi Time Scale Modeling for the Control Design of a Grid Connected Micro Turbine Generator by Power Electronic Converters, International Symposium on Industrial Electronics (IEEE-ISIE 2006), ETS-Downtown Montreal (Quebec), Canada, July 2006, CD-ROM.
- [10] P. Li, Ph. Degobert, B. François, B. Robyns, Power Control Strategy of a Photovoltaic Power Plant for Microgrid applications, ISES Solar World Congress 2007 (SWC 2007), Beijing, China, September 2007.